Fuentes-Paniagua, E., Hernández-Ros, J.M., Sánchez-Milla, M., Camero, M.A., Maly, M., Pérez-Serrano, J., Copa-Patiño, J.L., Sánchez-Nieves, J., Soliveri, J., Gómez, R. & Javier De La Mata, F. 2014, "Carbosilane cationic dendrimers synthesized by thiol-ene click chemistry and their use as antibacterial agents", RSC Advances, vol. 4, no. 3, pp. 1256-1265.

.

Available at http://dx.doi.org/10.1039/c3ra45408h

Carbosilane Cationic Dendrimers Synthesized by Thiol-Ene Click Chemistry and Their Use as Antibacterial Agents

Elena Fuentes-Paniagua,[a], [b] José Manuel Hernández-Ros[c], María Sánchez-Milla, [a], [b] M. Alejandra Camero,[a] Marek Maly,[d] Jorge Pérez-Serrano,[c]José Luis Copa-Patiño,[c] Javier Sánchez-Nieves, [a], [b] Juan Soliveri,[c] Rafael Gómez, [a], [b],* F. Javier de la Mata, [a], [b],*

[a] Departamento de Química Orgánica y Química Inorgánica, Universidad de Alcalá, Campus Universitario, E-28871 Alcalá de Henares (Spain); javier.delamata@uah.es;

[b] Networking Research Center on Bioengineering, Biomaterials and Nanomedicine (CIBER-BBN), Spain; FAX: (+34) 91 885 4683; e-mail: rafael.gomez@uah.es;

[c] Departamento de Biomedicina y Biotecnología, Universidad de Alcalá, Campus Universitario, E-28871, Alcalá de Henares, Spain; e-mail: juan.soliveri@uah.es

[d] Faculty of Science, J. E. Purkinje University, Ceske mladeze 8, 400 96 Usti n. L., Czech Republic.

Abstract

Cationic carbosilane dendrimers of generations 1-3 have been synthesized employing thiol-ene click chemistry. The obtained dendrimers present three different types of ammonium functions, two of them with the charge at the surface, $-NH_3^+$ and $-NMe_3^+$, and other with the charge internalized by the presence of ethylalcohol moieties, $-[NMe_2(CH_2CH_2OH)]^+$. The influence of $-NMe_3^+$ and $-[NMe_2(CH_2CH_2OH)]^+$ in dendrimer structure have been studied by molecular dynamics. The antibacterial properties of these families of dendrimers have been evaluated against Gram-positive (*Staphylococcus aureus* CECT 240) and Gram-negative (*Escherichia coli* CECT 515) bacterial strains, and the results obtained have been compared with those obtained for related cationic carbosilane dendrimers functionalized by hydrosilylation reactions. These data stand out the relevance of the sulfur atom *versus* the silicon atom close to the dendrimer surface and the outer charge versus the inner charge. Finally, the stability of the most active first generation dendrimers *vs*. pH and temperature has also been studied.

1. Introduction

The increasing occurrences of microbial antibiotic resistance[1] have prompted the search of alternatives to fight against infections. One of these alternatives is the use of quaternary ammonium salts (QAS), that have a broad spectrum of antimicrobial activity against both Gram-positive and Gram-negative bacteria.[2] Their antibacterial activity is based on the fact that the majority of bacterial cell walls are negatively charged, and hence interaction between ammonium compounds and cell walls destroy them.[3] Furthermore, other advantage of some QAS is their solubility in water, that allows them to kill bacteria in this medium.[4] Another approach to avoid resistance is the use of polymeric multifunctional antimicrobials.[5] The multivalency raises the activity of the functions attached to the macromolecule with respect to individual molecules. For biomedicine, this effect would lead to a stronger interaction of the dendrimer with its surrounding and this property has found a variety of applications.[6-13] Other advantages of these systems when compared with small-molecule antimicrobial agents are non volatility, chemical stability, long-term antimicrobial activity.[14]

The combination of QAS with macromolecules generates polycations that present high superficial charge. Different types of these macromolecules such as polymers,[14] dendrimers,[15] and hyperbranched polymers[16] have been studied as antimicrobial agents, exhibiting high antimicrobial activity due to their polivalency. The activity and mechanism of antimicrobial polycations could be affected by several factors such as molecular weight, polydispersity, spacer length between active site and main scaffold, hydrophilic-hydrophobic balance, and nature of counterions.[5,17]

In our research group we have previously synthesized carbosilane dendrimers and hyperbranched polymers, which are interesting not only because of their chemical and thermal stability, but also for their inert framework and biocompatibility. We have studied their activity in different biomedical applications,[18-20] including their antibacterial properties.[21,22] However, we have found as main drawback of these systems the synthetic procedure to decorate the macromolecules, which involves several steps starting from the basic carbosilane olefin structures. First, hydrosilylation with chlorosilanes that often

requires strictly controlled reaction conditions and are typically volatile and highly moisture sensitive, then substitution of Si-Cl bonds with Si-H bonds employing $LiAlH_4$ and finally hydrosilylation of the required allylamine, with the inherent problems of this type of reactions. For these reasons, new functionalization routes that would allow keeping the main structure of these compounds while avoiding the most difficult steps of the synthetic procedure, have become necessary.

The reactions of sulfur containing compounds with alkenes known as "thiol-ene chemistry",[23,24] are attractive due to their click characteristics,[25] easy initiation, high-yields, minimal product purification, and high tolerance to a variety of solvents and functional groups. This methodology has been employed in polymer functionalization and macromolecular synthesis,[25-29] including dendrimers.[30-33] For example, Son and coworkers have reported the synthesis of carbosilane dendrimers *via* thiol-ene reactions[34,35] and the functionalization of tetravinylsilane with a variety of thiols.[36] Related carbosilane dendrimers were obtained previously by nucleophilic substitution of chloromethyl groups with thiolates by Krska and Seyferth.[37]

The aim of the present research was to assess the antimicrobial activities of new carbosilane dendrimers synthesized by thiol-ene click reactions. These new dendrimers present different types of cationic functions, $-NH_3^+$, $-NMe_3^+$, and another with the charge internalized by the presence of ethylalcohol moieties, $-[NMe_2(CH_2CH_2OH)]^+$. This last group was chosen to maintain the solubility of the carbosilane dendrimers, as the high hydrophobicity of the carbosilane framework would probably lead to very low or insoluble dendrimers if the charge is hidden from the surface. The structures of dendrimers with $-NMe_3^+$ and $-[NMe_2(CH_2CH_2OH)]^+$ groups were studied by molecular dynamics to determine any differences between both cationic functions that could affect their behaviour. The antibacterial properties of these systems were also studied and compared with related cationic dendrimers that present a Si atom close to the ammonium groups (*i.e.* the hydrosilylation approach)[21,38] instead of S atoms (*i.e.* the thiol-ene approach). We believe that the incorporation of sulfur atoms close to the surface of the macromolecules would improve the antibacterial properties because it is known that natural and synthetic organosulfur

compounds possess important antibiotic properties, being employed for treatment of microbial and parasitic infections.[39-41]

2. Results and Discussion

2.1. Synthesis and characterization of dendrimers.

To carry out the thiol-ene reactions for obtaining the adequate cationic carbosilane dendrimers, we have first synthesized spherical dendrimers functionalized with vinyl groups at the periphery derived from 1,3,5-$C_6H_3(OH)_3$. The procedure employed has been the same that the previously reported for analogues dendrimers with allyl groups,[42] but using vinyl terminated dendrons[43] that were coupled to the polyphenoxo core (see Supporting Information). The reason to introduce vinyl instead of allyl moieties was the higher reactivity of these groups toward the thiol-ene addition, as we have also observed in similar dendrons. These new compounds $G_nO_3V_m$ (n = 1, m = 6 (**1**); n = 2, m = 12 (**2**); n = 3, m = 24 (**3**)) were characterized by NMR spectroscopy, MALDI-TOF and elemental analysis. The nomenclature employed for dendrimers described in this paper is of the type $G_nO_3X_m$, where G_n indicates generation, O_3 core derived from 1,3,5-$(HO)_3C_6H_5$, and X_m describe peripheral functions (X) and its number (m). The NMR spectra of the vinyl dendrimers **1**-**3** showed the characteristic signals of this group, two multiplets at δ 5.70 and 6.05 ppm in the ^{1}H NMR (Figure 1) and two resonances at δ 133.0 and 137.0 ppm in the ^{13}C NMR spectra. In the ^{1}H-^{29}Si HMBC spectra, one crosspeak for the Si atom bound to the vinyl groups was observed at δ -13.5. On the other hand, very clean MALDI-TOF spectra were obtained for the **1**-**3** vinyl dendrimers, with fine peaks centered at *m/z* values matching those for the calculated proton adducts.

Dendrimers decorated with ammonium functions were synthesized by thiol-ene reactions of the corresponding vinyl-terminated dendrimers $G_nO_3V_m$ **1**-**3** with commercially available aminoethanethiol hydrochloride or 2-(dimethylamino)ethanethiol hydrochloride (Scheme 1). The reactions were carried out under UV irradiation (365 nm) using a solvent mixture of THF/MeOH, a 1/1.2 thiol/alkene ratio, and with the presence of the radical initiator 2,2-dimethoxy-2-diphenylacetophenone (DMPA) in 5 % molar ratio with respect to thiol groups. After *ca*. 5 h. the new cationic carbosilane dendrimers $G_nO_3(SNH_3Cl)_m$ (n = 1,

m = 6 (**4**); n = 2, m = 12 (**5**); n = 3, m = 24 (**6**)) and $G_nO_3(SNMe_2{\cdot}HCl)_m$ (n = 1, m = 6 (**7**); n = 2, m = 12 (**8**); n = 3, m = 24 (**9**)) were obtained (Figure 2). These systems **4-9** were isolated as white solids in high yields (over 80 %), soluble in water and other polar solvents as alcohols and DMSO.

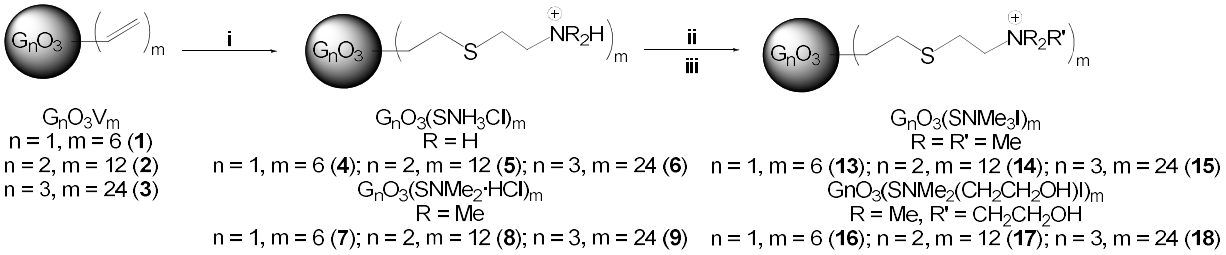

$G_nO_3V_m$
n = 1, m = 6 (**1**)
n = 2, m = 12 (**2**)
n = 3, m = 24 (**3**)

$G_nO_3(SNH_3Cl)_m$
R = H
n = 1, m = 6 (**4**); n = 2, m = 12 (**5**); n = 3, m = 24 (**6**)
$G_nO_3(SNMe_2{\cdot}HCl)_m$
R = Me
n = 1, m = 6 (**7**); n = 2, m = 12 (**8**); n = 3, m = 24 (**9**)

$G_nO_3(SNMe_3I)_m$
R = R' = Me
n = 1, m = 6 (**13**); n = 2, m = 12 (**14**); n = 3, m = 24 (**15**)
$GnO_3(SNMe_2(CH_2CH_2OH)I)_m$
R = Me, R' = CH_2CH_2OH
n = 1, m = 6 (**16**); n = 2, m = 12 (**17**); n = 3, m = 24 (**18**)

Scheme 1. Synthesis of cationic carbosilane dendrimers (counter anions have been omitted for clarity); i) $HS(CH_2)_2NR_2{\cdot}HCl$ (R = H, Me), DMPA, hν; ii) NaOH; iii) R'I (R' = Me, r. t.; R' = CH_2CH_2OH, 60 ºC).

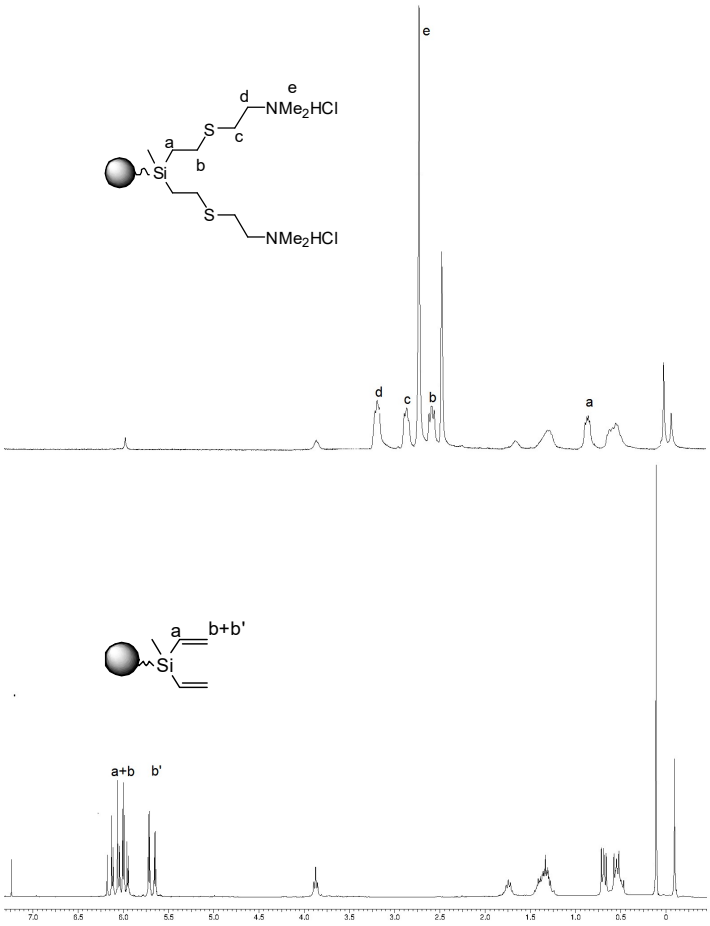

Figure 1. ^{1}H-NMR for compounds **8** in DMSO-d_6 (top) and **2** in $CDCl_3$ (bottom).

Structural characterization of dendrimers **4-9** has been carried out using elemental analysis, ^{1}H, ^{13}C, ^{15}N and ^{29}Si-NMR spectroscopy and mass spectrometry. The NMR spectroscopic and analytical data for derivatives **4-9** were consistent with their proposed structures (Figure 2). The ^{1}H and ^{13}C-NMR spectra in DMSO showed for the carbosilane framework identical chemical shifts for analogous nuclei in different generations. The formation of the new branches -$SiCH_2CH_2SCH_2CH_2N$- was clearly shown in the ^{1}H spectra by means of the triplets at δ *ca*. 0.87 and 2.60, for the inner methylene groups bonded to the silicon (a) and sulfur (b) atoms respectively, and by means of the triplets at δ *ca*. 2.76 and 2.94 (**4-6**) or 3.18 (**7-9**), for the outermost methylene groups bonded to the sulfur (c) and nitrogen (d) atoms. This observation was supported by data from COSY experiments. In the case of dendrimers **4-6** the protons directly bonded to the N atoms were observed as a broad singlet around δ 8.17, whereas for compounds **7-9** these protons appeared at δ *ca.* 11.1 and the methyl groups of the NMe_2H groups were observed at δ *ca*. 2.74. The $^{13}C\{^{1}H\}$-NMR spectra showed a signal around δ 41.3 corresponding to the methyl carbons of the NMe_2H functions (e) (compounds **7-9**) and a resonance at δ *ca*. 38.4 (**4-6**) or 55.2 (**7-9**) for the methylene bonded to the nitrogen atoms (d). Two signals were observed for the two different CH_2S groups, one at δ *ca*. 24.5 and other at δ *ca*. 26.0 attributed to the external (c) and internal (b) methylene groups respectively (determined by ^{1}H-^{13}C-HMBC experiments), while the most external methylene carbon directly bonded to silicon atom (a) appears at δ *ca*. 13.6. The chemical shift of quaternized N atoms were detected in ^{1}H-^{15}N NMR spectra by means of the resonances at δ *ca*. -342.4 (**4-6**) and at δ *ca*. -338.2 (**7-9**). ^{29}Si NMR spectroscopy (^{1}H-^{29}Si-HMBC) clearly support the disappearance of the starting vinyl groups, appearing a new resonance at δ *ca*. 2.5 for the new outermost silicon atom $Si(CH_2)_2S$.

In order to synthesize dendrimers with cationic NMe_3^+ and $[NMe_2(CH_2CH_2OH)]^+$ moieties (Scheme 1), first we proceeded to neutralize dendrimers **7-9**. Thus, addition of excess NaOH to these dendrimers allowed us to obtain the corresponding dimethylamine functionalized dendrimers $G_nO_3(SNMe_2)_m$ (n = 1, m = 6 (**10**); n = 2, m = 12 (**11**); n = 3, m = 24 (**12**)). These compounds were isolated in good yield (over 80

%) as pale yellow oils soluble in a variety of organic solvents, ethers, halogenated solvents, alcohols, DMSO, etc, but not in water. In general, the NMR data were very similar to those obtained for the parent compounds. The main differences were those related with the chemical change in the N atoms. In the ^{1}H NMR spectra, the NMe_2 and CH_2N groups were shifted to lower frequency, δ *ca*. 2.25 and 2.55 respectively. The same behaviour was observed in the ^{13}C NMR spectra for the C atoms of these groups (δ *ca*.45.2 and δ *ca*. 59.1) and for the chemical shift of the N atoms in the ^{1}H-^{15}N NMR spectra (δ *ca*. -352.1). However, the chemical shift of silicon atoms was not affected due to the distance to the N atoms.

From compounds **10**-**12** and by addition of excess MeI or $HO(CH_2)_2I$ we have obtained the new ammonium-terminated dendrimers $G_nO_3(SNMe_3I)_m$ (n = 1, m = 6 (**13**); n = 2, m = 12 (**14**); n = 3, m = 24 (**15**)) or $G_nO_3[SNMe_2(CH_2CH_2OH)I]_m$ (n = 1, m = 6 (**16**); n = 2, m = 12 (**17**); n = 3, m = 24 (**18**)), respectively, in good yields (over 80%) as solids soluble in water, alcohols and DMSO (Figure 2). For compounds $G_nO_3(SNMe_3I)_m$ (**13**-**15**) the reaction was carried out at ambient temperature for 16 hours whereas for compounds $G_nO_3(SNMe_2(CH_2CH_2OH)I)_m$ (**16**-**18**) heating at 60 ºC for 3 days was necessary. Structural characterization of dendrimers **13**-**18** has been carried out using elemental analysis, ^{1}H, ^{13}C, ^{15}N and ^{29}Si-NMR spectroscopy and mass spectrometry.

The presence of the ammonium functions was confirmed in the ^{1}H NMR spectra by the resonance corresponding to the methyl substitution of the NMe groups over δ 3.11 and in the ^{13}C NMR spectra about δ 53.7, shifted to higher frequency with respect to the neutral dendrimers **10**-**12**. The chemical shift corresponding to these N atoms was observed at δ *ca*. -330.0 (**13**-**15**) and δ *ca*. -324.2 (**16**-**18**), as consequence of the presence of the positive charge on the nitrogen atom. MS-ESI technique was used to determine $[M-(m\ I)]^{m+}$ peaks of dendrimers $G_nO_3(SNMe_3I)_m$ (**13**-**15**) and $G_nO_3(SNMe_2(CH_2CH_2OH)I)_m$ (**16**-**18**) (See experimental part).

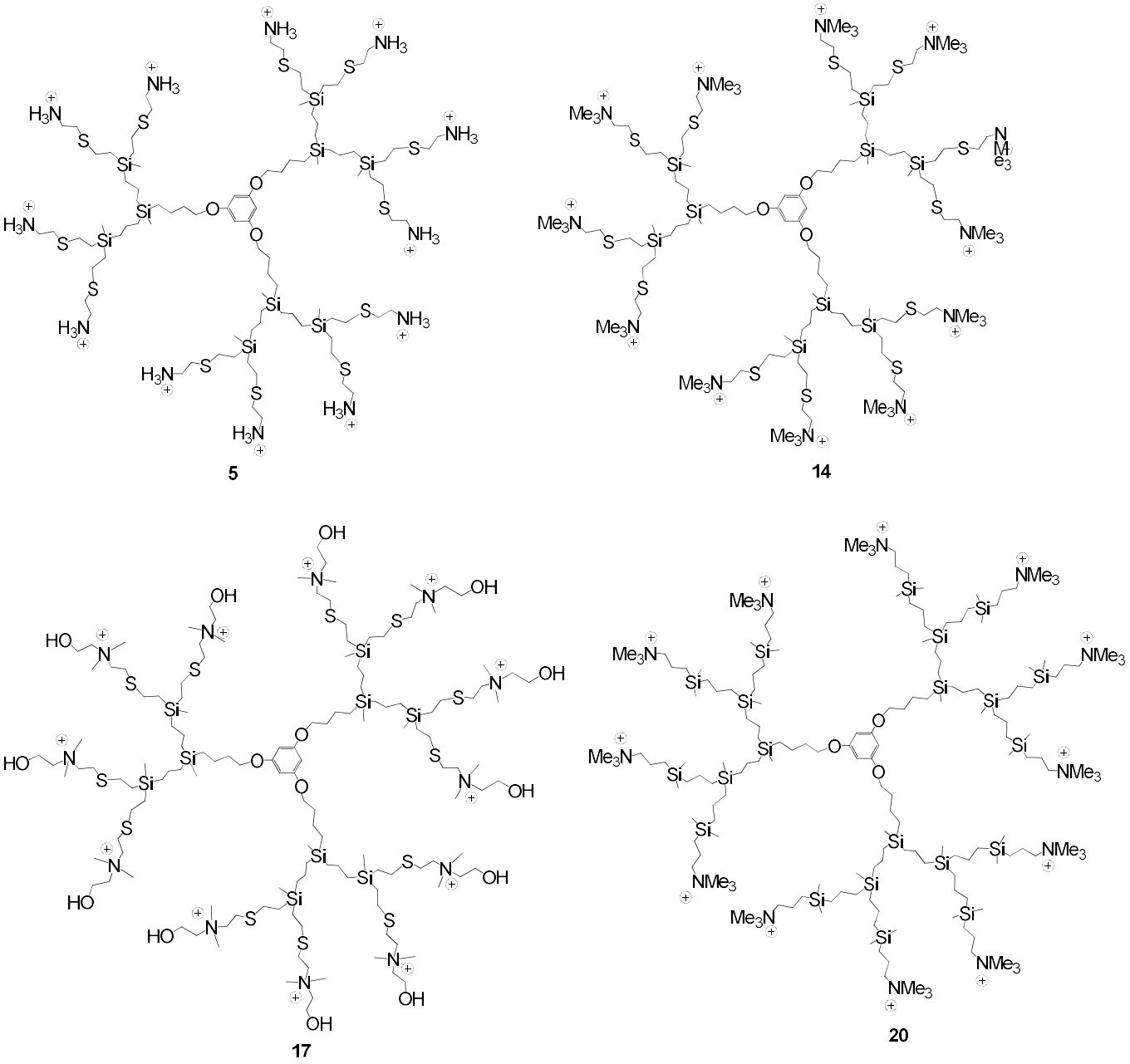

Figure 2. Drawing of cationic dendrimers of second generation used in this work.

2.3. Computer modeling.

Computer models of the second generation cationic dendrimers **14** and **17** were created and simulated in explicit salt water using molecular dynamics in order to get detail information about their size and conformations in water environment, considering physical conditions: T = 310 K, P = 0.1 MPa. The most representative dendrimer structures from the last 30 ns of the total 65 ns long simulation have spherical

shape with rather excentrically positioned core polyphenol ring (Figure 3). Equilibrated dendrimer structures were consequently analyzed. Only slightly higher values of radius of gyration (Rg) and maximal distance of the dendrimer atoms from the dendrimer center of geometry (Rmax) were obtained for dendrimer **17** than for **14** (Rg = 10.0 Å (**14**), 10.6 Å (**17**); Rmax = 18.0 Å (**14**), 19.1 Å), as consequence of the presence of the $-(CH_2)_2OH$ chain.

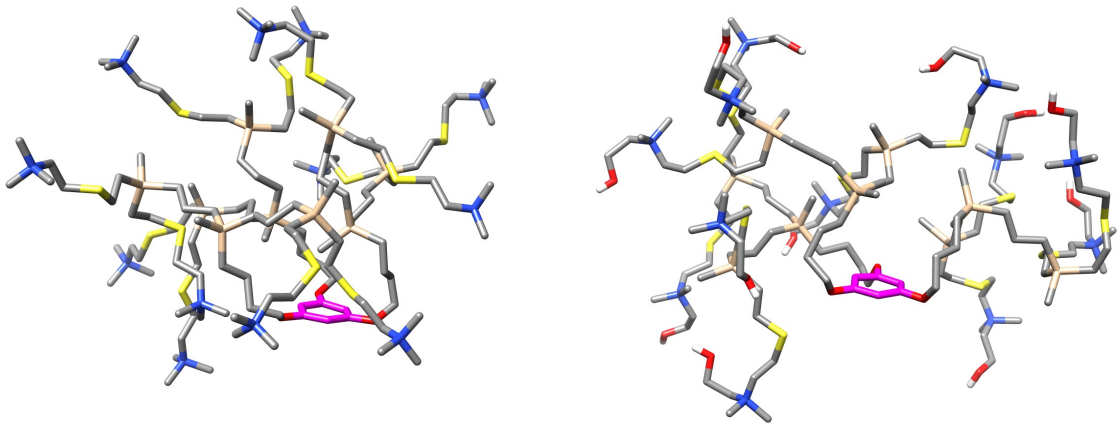

Figure 3. Computer models of dendrimers **14** (left), **17** (right). Hydrogen atoms are omitted for the better clarity (except those from OH groups). The most representative conformations from the last 30 ns of simulation are shown. Polyphenol ring carbon atoms are colored in magenta. Colors of all remaining atoms are: C – grey, O – red, Si – beige, S – yellow.

The radial distribution function (RDF) of both dendrimers (**14**, **17**) is helpful to analyze more in detail and more clearly some differences between them (Figure 4). The radial densities of N atoms of **14** and **17** have similar shapes and from *ca.* 8 Å are nearly identical. Both profiles have their maximum at 4.7 Å with 0.2 Å precision, which indicates presence of backfolding (Figure S4, Supporting Information). It is more intensive in case of structure **17**, as can be seen from the significantly higher maximal peak.

In the case of dendrimer **17**, it is also interesting to compare the profiles of terminal N and O atoms. First of all, the O-profile has a significantly smaller maximal peak, in spite of the fact that each terminal oxygen atom is attached through just two-carbon spacer to the given nitrogen atom. However, this spacer gives to oxygen atoms some more degrees of freedom (comparing to N atoms) and this is reflected in a

smaller maximal peak. On the other hand, the average density of terminal oxygen atoms in longer distances region, i.e. area of non-backfolded terminal units (from *ca.* 17.7 Å to *ca.* 22 Å), is higher than density of nitrogen atoms. This datum indicates that at least some oxygen atoms are not "backfolded" (carbon spacer is not bent), but that they rather form an outer portion of the molecular surface, being the -OH groups fully disposal for eventual interaction with another molecules (proteins, nucleic acids, etc.).

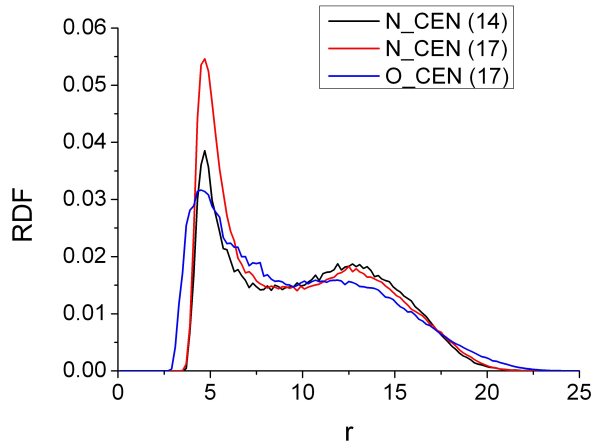

Figure 4. Radial distribution density profiles of N and terminal O atoms (those from OH groups) with respect to C atoms from polyphenol ring. Numbers in parentheses denote given dendrimer.

The effect of $-NMe_3^+$ and $-[NMe_2(CH_2CH_2OH)]^+$ groups in the external charge of dendrimers **14** and **17** was calculated and visualized by electrostatic potential on the molecular surface (Figure 5). In the case of dendrimer **17** it is observed slightly more frequent red spots indicating lower potential values, due to the presence of the most electronegative oxygen atoms sufficiently close to the molecular surface. However, the effect of higher local electron density around oxygen atoms is of course not so high as obviously surrounding attached atoms have lower electron density. Also, the dipole character of -OH moieties can be detected on the molecular surface if they are oriented properly (Figure S5, Supporting Information).

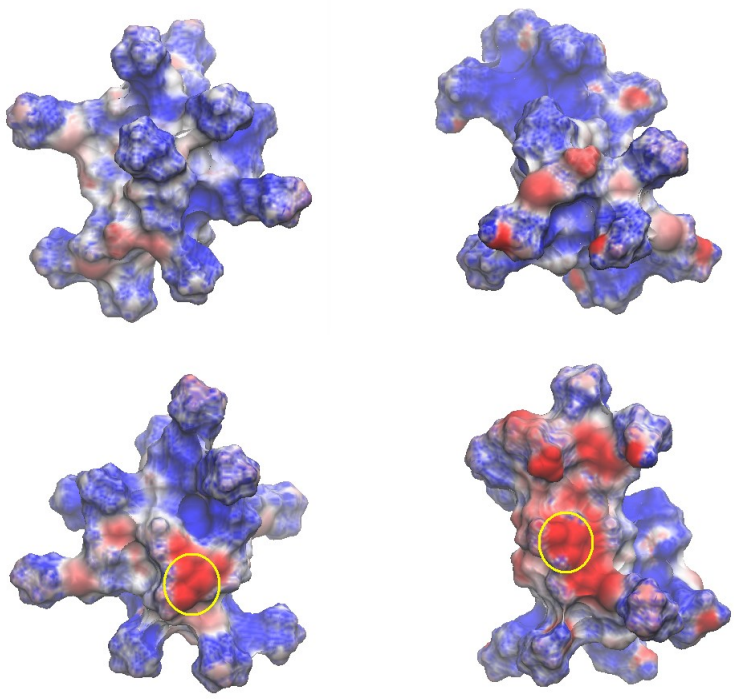

Figure 5. Molecular surface of dendrimer models **14** (left) and **17** (right) colored according to electrostatic potential. The same conformations as those shown in Figure 3 were used here. Top view (top), bottom view (bottom). Red color denotes low values (+5 kT/e (0.128 V) and lower) and the blue color means high potential values (+10 kT/e (0.256 V) and higher). The effect of water was implicitly taken into account in this electrostatic calculation. The yellow circle indicates position of polyphenol ring.

To compare direct interaction of cationic terminal units of both dendrimers with anionic moieties we calculated also radial density profiles of Cl^- anions with respect to N atoms (Figure 6). In both dendrimers, the Cl^- ion stabilized for a while by electrostatic interaction with the given cationic group is located at *ca*. 5 Å from the N atom. The noticeable higher maxima of dendrimer **14** might be connected mainly with better accessibility of the cationic charge (more suitable positions of Cl^- anions at distance 5 Å from the central N atom are available) and eventually also with slightly stronger interaction due to smaller differences in local charge distribution than in dendrimer **17**. Another difference between these compounds is that in the case of dendrimer **17** it is distinguished a second maxima (at *ca*. 6 Å) comparable with the first one, which involves interaction with the -OH dipole (Figure S6, Supporting Information).

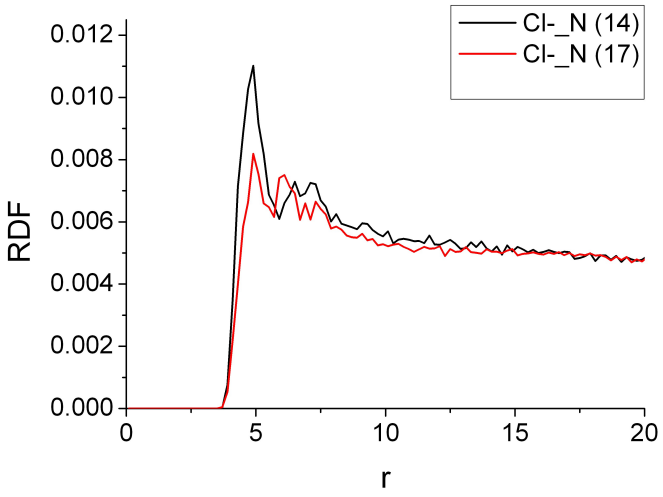

Figure 6. Radial distribution density profiles of Cl^- ions with respect to N atoms. Numbers in parentheses denote given dendrimer.

2.3. Antibacterial activity.

The biocide effect of cationic dendrimers is due to the high local concentration of cationic charges, and thus we have decided to compare the activity of the dendrimers with different outer modifications described above. For this purpose we have measured the growth of S. *aureus* CECT 240, as a model of Gram+ bacterias, and E. *coli* CECT 515, as a model of Gram- bacterias, in the presence and absence of dendrimer, in order to check the comparative activity of dendrimers to produce membrane disruption in these strains.

The measuring of the minimum inhibitory concentration (MIC) and minimum bactericidal concentration (MBC) of these compounds (Table 1) have shown the influence of different parameters to take into account in the design of antibacterial polycationic compounds. First of all, we have compared the activity of cationic carbosilane dendrimers synthesized by thiol-ene reaction (**13**-**15**) with similar dendrimers obtained by hydrosilylation, $G_nO_3(SiNMe_3I)_m$ (n=1, m=6 (**19**); n=2, m=12 (**20**); n=3, m=24 (**21**))[38] (Figure 2), in order to observe the influence of the sulfur atoms close to the dendritic periphery. In this sense, it has been found that the presence of the sulfur atom improves significantly the biocidal effect of these compounds, especially in the case of E. *coli* CECT 515 (Table 1). These results make the thiol

derivatives **13-15** good candidates for this purpose, as disruption of Gram- bacterias is more complicated due to the presence of an extra layer in comparison to Gram+ bacterias, which just contain a thick peptidoglycan layer. It is important to highlight that biocidal activity decreases, in general, when dendritic generation increased. As biocidal activity of these types of compounds depends basically on two factors, the number of quaternized groups and the biopermeability processes, which depend on size and the presence of lipophilic domains, we can assume that for dendrimers **13-15** and **19-21** the second factor has more influence.

On the other hand, to study the influence of nitrogen substituyents, we have measured the biocidal activity of dendrimers that present different peripheral ammonium groups, as $-NH_3^+$ (**4-6**), $-NMe_3^+$ (**13-15**), and; $-[NMe_2(CH_2CH_2OH)]^+$ (**16-18**). In general, the charge internalization has a negative effect in the activity of these dendrimers (Table 1), indicating a diminishing of the interaction between dendrimers and bacterias, in accordance with theoretical data (see above) and with previously published results.[44] The anomalous behaviour of third generation dendrimer **6** is attributed to solubility and aggregation problems.

Compound		**4**	**5**	**6**	**13**	**14**	**15**	**16**	**17**	**18**	**19**	**20**	**21**	PenVK
S. *aureus* CECT 240	MIC	2	4	32	2	2	8	2	4	16	2	8	16	0.01
	MBC	2	4	32	2	2	8	8	8	32	2	8	16	0.31
E. *coli* CECT 515	MIC	2	8	128	2	8	16	4-8	8	64	16	64	64	256
	MBC	2	8	128	4	8	16	8	8	64	32	64	64	256

Table 1. Bacteriostatic (MIC) and bactericide (MBC) concentrations of dendrimers discussed in this work and PenVK (all concentrations data are measured in mg L^{-1}).

The comparison of the data obtained from dendrimers with the antibiotic penicillin V potassium salt (PenVK ,Table 1), an effective antibiotic against Gram-positive but not against Gram-negative bacteria, indicates that dendrimers are much more active against Gram-negative bacteria than penicillin, whereas their activity is similar against Gram-positive bacteria (this can be better observed when the MBC is measured as μM concentration, data don´t shown). However, these systems can be considered as broad

spectrum biocides, as the values found for the multivalent dendrimer systems are close for both type of bacterias.

One drawback of penicillins is their high instability against pH due to the presence of a β-lactam ring in their structure. For this reason we have performed a stability study of dendrimers toward variations of pH and temperature. For this purpose we have employed a response surface methodology using a three factor, three-level Box-Behnken design to analyze the effect of three variables in the stability of the dendrimers. The independent variables used in this design were: temperature (20-60ºC), pH (5-9 units pH) and incubation time of the dendrimer at different temperatures and pHs (6-48 hours). For this study we have chosen first generation compounds with $–NMe_3^+$ groups on their periphery obtained by thiol-ene click chemistry (**13**) and by hydrosilylation (**19**). We have discarded dendrimer **4**, although it showed analogous activity, due to the presence of acid $–NH_3^+$ groups in its periphery that makes this compound instable in basic media, leading to the precipitation of a neutral dendrimer, $G_1O_3(SNH_2)_6$. This behaviour was confirmed by pH titration and the results compared with those obtained theoretically (see Supporting Information).

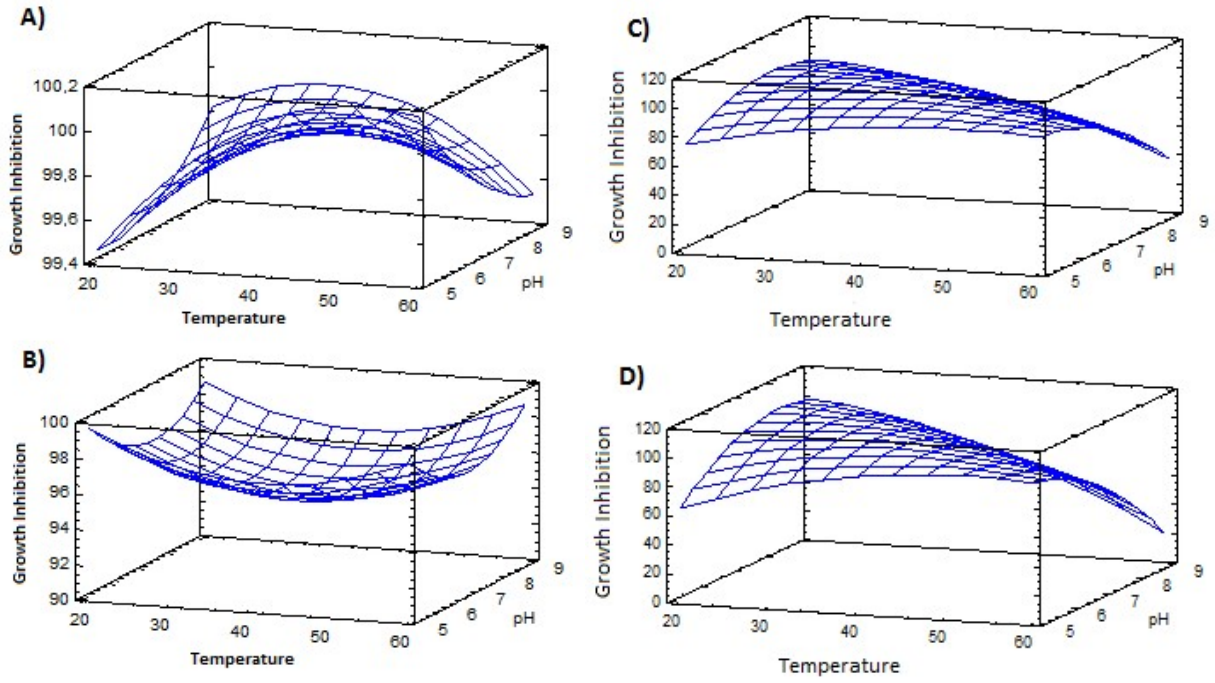

Figure 7. Stability assay for **19** against E. *coli* CECT 515 (A) and S. *aureus* CECT 240 (B), and stability assay for **13** against E. *coli* CECT 515 (C) and S. *aureus* CECT 240 (D). The third variable studied (time of incubation of the dendrimer at different temperatures and pHs) is 27 hours in the graphs.

The stability study of compound **19** against pH, time and temperature showed that the activity of this compound is kept in all the measured conditions as is shown in Figure 7 (near 100 % growth inhibition). However, in the case of dendrimer **13**, its activity decreased in basic medium. We believe that this is probably due to a very small decomposition of the outer functions due to Hofmann's elimination. As this process consists in the abstraction of a hydrogen atom from β-position with respect to the ammonium group by the hydroxide anion, the presence of a sulfur atom also in this β-position could probably enhance this decomposition. Unfortunately we have not been able to observe any modification of the NMR spectra of compound **13** when treated in these conditions, although any small change in the dendrimer surface may alter their antibacterial activity.

3. Conclusions

The combination of thiol-ene click reactions and quaternization with iodo-derivatives is a convenient methodology for the functionalization of carbosilane dendrimers with different ammonium groups. Thus, following this procedure we have synthesized cationic carbosilane dendrimers with $-NH_3^+$, $-NMe_3^+$, and, $-[NMe_2(CH_2CH_2OH)]^+$ groups.

The structures of cationic dendrimers **14** and **17**, with $-NMe_3^+$ and $-[NMe_2(CH_2CH_2OH)]^+$ groups respectively, were studied by computer modeling. The presence of hydroxyl groups in dendrimer **17** gives rise to slightly lower electrostatic potential on its surface and worse accessibility of the cationic charge. On the other hand, the OH dipoles to interact with anionic centers on the given dendrimer receptor, we can expect a better interaction of dendrimer **14** with proteins as those that form part of bacterial membranes, and thus higher destabilization can be produced.

These cationic dendrimers and the analogous dendritic systems obtained through hydrosilylation with peripheral -NMe_3^+ moieties were studied as antimicrobial agents against Gram-positive (*Staphylococcus aureus* CECT 240) and Gram-negative (*Escherichia coli* CECT 515) bacterial strains. In general, the bactericide activity decreases with increasing generations. The results also showed a positive effect of the sulfur atom close to the surface with respect to those with a Si atom, being this effect more relevant in the case of gram-negative bacterias, which are also more resistant bacterias to antibiotics due to the presence of a double layer membrane. With respect to the different types of ammonium groups, the activity decreases when the size of nitrogen substituyents increases, as consequence of charge internalization that diminishes the interaction with the bacterial membrane. This supposition is in accordance with the results obtained from theoretical calculations. However, whereas the presence of a sulfur atom close to the nitrogen atoms enhances the antibacterial activity, this sulfur atom affects negatively the stability of thiol-ene dendrimers in basic medium.

Although the presence of the –OH moieties diminishes antibacterial activity, these groups could reinforced other type of interactions through hydrogen-bonding or also be used as a linker unit by formation of ester bonds with molecules of pharmacological interest. These possibilities are being now considered for ongoing studies.

4. Experimental Section

4.1. General Considerations. All reactions were carried out under inert atmosphere and solvents were purified from appropriate drying agents when necessary (THF). NMR spectra were recorded on a Varian Unity VXR-300 (300.13 (^{1}H), 75.47 (^{13}C) MHz) or on a Bruker AV400 (400.13 (1H), 100.60 (^{13}C), 40.56 (^{15}N), 79.49 (^{29}Si) MHz). Chemical shifts (δ) are given in ppm. ^{1}H and ^{13}C resonances were measured relative to internal deuterated solvent peaks considering TMS = 0 ppm, meanwhile ^{15}N and ^{29}Si resonances were measured relative to external MeNO and TMS, respectively. When necessary, assignment of resonances was done from HSQC, HMBC, COSY, TOCSY and NOESY NMR experiments. Elemental analyses were performed on a LECO CHNS-932. Mass Spectra were obtained from a Bruker Ultraflex III

and an Agilent 6210. Thiol-ene reactions were carried out employing a HPK 125 W mercury lamp from Heraeus Noblelight with maximum energy at 365 nm, in normal glassware under an inert atmosphere. Compounds, $HS(CH_2)_2NH_2{\cdot}HCl$, $HS(CH_2)_2NMe_2{\cdot}HCl$, 2,2'-dimethoxy-2-phenylacetophenone (DMPA), MeI (Aldrich) and K_2CO_3 (Panreac) were obtained from commercial sources. Compounds $G_nO_3(NMe_3I)_m$[38] were synthesized as published.

4.2. Synthesis of selected compounds.

$G_1O_3V_6$ (1). 1,3,5-$(HO)_3C_6H_3$ (0.36 g, 2.86 mmol), BrG_1V_2 (2.00 g, 8.57 mmol), K_2CO_3(2.37 g, 17.15 mmol) and crown ether 18-C-6 (0.23 g, 0.86 mmol) were stirred in acetone (70 mL) at 90ºC into a sealed ampoule for 3 days under vacuum. Afterward, volatiles were removed under vacuum and a water solution of NH_4Cl (12%, 50 mL) and Et_2O were added. The organic phase was separated and the aqueous phase was extracted twice with Et_2O. The organic phase was dried over $MgSO_4$ and for extra 10 min also with SiO_2. The solution was filtered and the volatiles were removed under vacuum, yielding **1** as colorless oil (1.500 g, 90 %). Data for **1**: NMR ($CDCl_3$): ^{1}H-NMR: δ 0.13 (s, 9 H, Si*Me*C_2H_3), 0.69 (m, 6 H, C*H*$_2$SiC_2H_3), 1.47 (m, 6 H, $OCH_2CH_2CH_2CH_2Si$), 1.76 (m, 6 H, $OCH_2CH_2CH_2CH_2Si$), 3.88 (t, J = 6.6 Hz, 6 H, $OCH_2CH_2CH_2CH_2Si$), 5.70 and 6.07 (m, 21 H, Si*CHCH*$_2$ and $C_6H_3O_3$). ^{13}C-NMR: δ -7.1 (Si*Me*), 13.7 ($OCH_2CH_2CH_2CH_2Si$), 20.3 ($OCH_2CH_2CH_2CH_2Si$), 29.2 ($OCH_2CH_2CH_2CH_2Si$), 67.5 ($OCH_2CH_2CH_2CH_2Si$), 93.7 ($C_6H_3O_3$; *C*-H), 132.9 (Si*C*HCH$_2$), 136.8 (SiCH*C*H$_2$), 160.9 ($C_6H_3O_3$; *C*-O). ^{29}Si-NMR: δ -13.5 (*Si*CHCH$_2$). Anal. Calc. $C_{33}H_{54}O_3Si_3$ (583.04 g/mol): C, 67.98; H, 9.34; Exp.: C, 67.24; H, 9.40. MS: $[M + H]^+$= 583.35 uma (calcd. = 583.35 uma).

$G_1O_3(SNH_3Cl)_6$ (4). Dendrimer **1** (0.200 g, 0.34 mmol), cysteamine hydrochloride (0.260 g, 2.30 mmol), 5 % molar of DMPA (0.016 g, 0.06 mmol), and a 1:2 THF/methanol solution (5 ml).The reaction mixture was deoxygenated and irradiated for 1.5 h. Another 5 % molar DMPA was added and the reaction mixture was irradiated for another 1.5 h and monitored by ^{1}H-NMR. The initial reaction mixture was concentrated via rotator evaporation and solved in water. Then, nanofiltration with membranes of MW = 500 was performed. The pure product was dried in vacuo to afford **4** as a white solid (0.140 g, 60%). Data

for **4**: NMR (DMSO): ^{1}H-NMR: δ -0.02 (s, 9 H, Si*Me*), 0.61 (t, 6 H, $OCH_2CH_2CH_2CH_2$SiMe), 0.87 (t, 12 H, -SiCH_2CH_2S), 1.40 (m, 6 H, $OCH_2CH_2CH_2CH_2$SiMe), 1.69 (m, 6 H, $OCH_2CH_2CH_2CH_2$SiMe), 2.75 (t, 12 H, -SiCH_2CH_2S), 2.77 (t, 12 H, S$CH_2CH_2NH_3^+$), 2.93 (t, 12 H, S$CH_2CH_2NH_3^+$), 3.90 (t, 6 H, O$CH_2CH_2CH_2CH_2$SiMe), 6.03 (s, 3 H,$C_6H_3O_3$), 8.10 (s, 3 H, -NH_3^+). ^{13}C-NMR: δ -5.4 (Si*Me*), 12.7 ($OCH_2CH_2CH_2CH_2$SiMe), 13.9 (-SiCH_2CH_2S), 19.7 ($OCH_2CH_2CH_2CH_2$SiMe), 26.3 (-SiCH_2CH_2S), 27.7 (S$CH_2CH_2NH_3^+$), 32.4 ($OCH_2CH_2CH_2CH_2$SiMe), 38.4 ($SCH_2CH_2NH_3^+$), 67.0 (O$CH_2CH_2CH_2CH_2$SiMe), 93.6 ($C_6H_3O_3$, *C*-H), 160.5 ($C_6H_3O_3$, *C*-O). ^{15}N-NMR: δ -342.4 (-*N*H_3^+). ^{29}Si-NMR*:* 2.1 (SiMe). ESI: (1260.38 g/mol) q=2 (523.28 [M-4HCl-2Cl$^-$]$^{2+}$), q=3 (349.18 [M-3HCl-3Cl$^-$]$^{3+}$). Anal. Calc. $C_{45}H_{102}Cl_6N_6O_3S_6Si_3$ (1264.69 g/mol): C, 42.74; H, 8.13; N, 6.65; S, 15.21. Exp.: C, 39.21; H, 7.61; N, 6.42; S, 15.56.

$G_1O_3(SNMe_2HCl)_6$ (**7**). This dendrimer was prepared from **1** (0.374 g, 0.64 mmol), 2-(Dimethylamino)ethanethiol hydrochloride (0.631 g, 4.23 mmol), DMPA (0.100 g, 0.38 mmol), and a 1:2 THF/methanol solution (3 ml) using the preparative procedure for **4**. The pure product was dried in vacuo to afford **7** as a white solid (0.533 g, 58%). Data for **7**: NMR (DMSO): ^{1}H-NMR: δ 0.03 (s, 9 H, Si*Me*), 0.61 (m, 6 H, $OCH_2CH_2CH_2CH_2$Si), 0.88 (t, J_a = 8.3 Hz, 12 H, SiCH_2CH_2S), 1.40 (m, 6 H, $OCH_2CH_2CH_2CH_2$Si), 1.69 (m, 6 H, $OCH_2CH_2CH_2CH_2$Si), 2.61 (t, J_a = 8.7 Hz, 12 H, $SiCH_2CH_2$S), 2.71 (s, 36 H, $SCH_2CH_2NMe_2H^+$), 2.86 (t, J_b = 7.9 Hz, 12 H, S$CH_2CH_2NMe_2H^+$), 3.22 (t, J_a = 8.0 Hz, 12 H, $SCH_2CH_2NMe_2H^+$), 3.90 (m, 6 H, OCH_2), 6.03 (s, 3 H, $C_6H_3O_3$), 10.71 (bs, 6 H, -NMe_2H^+). ^{13}C-NMR: δ -5.8 (Si*Me*), 12.2 ($OCH_2CH_2CH_2CH_2$Si), 13.5 (SiCH_2CH_2S), 19.3 ($OCH_2CH_2CH_2CH_2$Si), 24.2 (S$CH_2CH_2NMe_2H^+$), 26.0 ($SiCH_2CH_2$S), 32.0 ($OCH_2CH_2CH_2CH_2$Si), 41.4 ($SiCH_2CH_2NMe_2H^+$), 55.3 ($SCH_2CH_2NMe_2H^+$), 66.5 (OCH_2), 93.1 ($C_6H_3O_3$; *C*-H), 159.9 ($C_6H_3O_3$; *C*-O). ^{15}N-NMR: δ -338.3 (-*N*Me_2H^+). ^{29}Si-NMR: δ 3.1 (G_1–*Si*Me). Anal. Calcd. $C_{57}H_{126}Nj_6Cl_6O_3S_6Si_3$ (1433.01 g/mol): C, 47.77; H, 8.86; N, 5.86; S, 13.43; Found: C, 46.62; H, 8.76; N, 5.90; S, 12.63.H.

$G_1O_3(SNMe_2)_6$ (**10**). In a $H_2O/CHCl_3$ (1:1, 20 ml) solution of **7** (0.265 g, 0.18 mmol), a NaOH solution was added drop by drop (0.055 g, 1.38 mmol). The reaction mixture was stirred for 15 minutes at room

temperature, and finally the aqueous phase was removed. The organic phase was dried in vacuo to get **10** as a pale yellow oil (0.224 g, 100%). Data for **10**: NMR ($CDCl_3$): ^{1}H-NMR: δ 0.01 (s, 9 H, Si*Me*), 0.60 (m, 6 H, $OCH_2CH_2CH_2CH_2Si$), 0.90 (t, J = 8.6 Hz, 12 H, $SiCH_2CH_2S$), 1.45 (m, 6 H, $OCH_2CH_2CH_2CH_2Si$), 1.75 (m, 6 H, $OCH_2CH_2CH_2CH_2Si$), 2.25 (s, 36 H, $SCH_2CH_2NMe_2$), 2.47 (m, 12 H, $SCH_2CH_2NMe_2$), 2.52 (m, 12 H, $SiCH_2CH_2S$), 2.59 (m, 12 H, $SCH_2CH_2NMe_2$), 3.85 (t, J = 6.3 Hz, 6H, OCH_2), 6.02 (s, 3H, $C_6H_3O_3$). ^{13}C-NMR: δ -5.4 (Si*Me*), 13.3 ($OCH_2CH_2CH_2CH_2Si$), 14.5 ($SiCH_2CH_2S$), 20.3 ($OCH_2CH_2CH_2CH_2Si$), 27.6 ($SCH_2CH_2NMe_2$), 29.8 ($SiCH_2CH_2S$), 33.0 ($OCH_2CH_2CH_2CH_2Si$), 45.4 ($SiCH_2CH_2NMe_2$), 59.2 ($SCH_2CH_2NMe_2$), 67.3 (OCH_2), 93.7 ($C_6H_3O_3$; *C*-H), 160.8 ($C_6H_3O_3$; *C*-O). ^{15}N-NMR: δ -352.1 (-*N*Me_2). ^{29}Si-NMR: δ 2.4 (G_1–*Si*Me). MS: $[M+H]^+$ = 1213.7 uma (calcd. = 1213.8 uma). Anal. Calcd. $C_{57}H_{120}N_6O_3S_6Si_3$ (1214.25 g/mol): C, 56.38; H, 9.96; N, 6.92; S, 15.84; Found: C, 55.68; H, 9.43; N, 6.77; S, 14.94.

$G_1O_3(SNMe_3I)_6$ (**13**). To a diethyl ether (20 ml) solution of **10** (0.198 g, 0.16 mmol) were added 0.05 ml of MeI solution (1.12 mmol). The resulting solution was stirred for 16 h at room temperature and then evaporated under reduced pressure and washed twice with hexane (20 ml). **13** is got after drying as a white solid (0.310 g, 93%). Data for **13**: NMR (DMSO): ^{1}H-NMR: δ 0.05 (s, 9 H, Si*Me*), 0.63 (m, 6 H, $OCH_2CH_2CH_2CH_2Si$), 0.88 (m, 12 H, $SiCH_2CH_2S$), 1.41 (m, 6 H, $OCH_2CH_2CH_2CH_2Si$), 1.69 (m, 6 H, $OCH_2CH_2CH_2CH_2Si$), 2.64 (m, 12 H, $SiCH_2CH_2S$), 2.89 (m, 12 H, $SCH_2CH_2NMe_3^+$), 3.09 (s, 36 H, $SCH_2CH_2NMe_3I$), 3.53 (m, 12 H, $SCH_2CH_2NMe_3^+$), 3.89 (t, 6 H, OCH_2), 6.02 (s, 3 H, $C_6H_3O_3$). ^{13}C-NMR: δ -6.4 (Si*Me*), 11.8 ($OCH_2CH_2CH_2CH_2Si$), 12.9 ($SiCH_2CH_2S$), 18.5 ($OCH_2CH_2CH_2CH_2Si$), 22.3 ($SCH_2CH_2NMe_3^+$), 25.5 ($SiCH_2CH_2S$), 31.4 ($OCH_2CH_2CH_2CH_2Si$), 51.0 ($SiCH_2CH_2NMe_3^+$), 63.3 ($SCH_2CH_2NMe_3^+$), 66.1 (OCH_2), 92.0 ($C_6H_3O_3$; *C*-H), 160.7 ($C_6H_3O_3$; *C*-O). ^{15}N-NMR: δ -330.0 (-*N*Me_3^+). ^{29}Si-NMR: δ 3.3 (G_1–*Si*Me). ESI: (2064.27 g/mol) q=2 (905.24 $[M-2I^-]^{2+}$), q=3 (561.18 $[M-3I^-]^{3+}$), q=4 (389.17 $[M-4I^-]^{4+}$). Anal. Calcd. $C_{63}H_{138}I_6N_6O_3Si_3$ (2065.88 g/mol): C, 36.63; H, 6.73; N, 4.07; S, 9.31; Found: C, 37.26; H, 6.67; N, 3.89; S, 8.46.

$G_1O_3(NMe_2(CH_2CH_2OH)I)_6$ (16). To a solution of **10** (0.183 g, 0.15 mmol) in THF (20 ml) 0.09 ml of $I(CH_2)_2OH$ solution (1.08 mmol) were added. The resulting solution was stirred at 60ºC into a sealed ampoule for 3 days in dark under argon. Then, the reaction mixture was evaporated under reduced pressure and washed once with dichloromethane (10ml) and once with hexane (10 ml). **16** is got after drying as a brownish solid (0.270 g, 80%). Data for **16**: NMR (DMSO): ^{1}H-NMR: δ 0.04 (s, 9 H, Si*Me*), 0.63 (t, 12 H, $OCH_2CH_2CH_2CH_2Si$), 0.88 (t, 12 H, $SiCH_2CH_2S$), 1.39 (m, 6 H, $OCH_2CH_2CH_2CH_2Si$), 1.73 (m, 6 H, $OCH_2CH_2CH_2CH_2Si$), 2.66 (t, 12 H, $SiCH_2CH_2S$), 2.91 (m, 12 H, $SCH_2CH_2N^+$), 3.11 (s, 36 H, -$NMe_2CH_2CH_2OHI$), 3.43 (m, 12 H, -$NMe_2CH_2CH_2OHI$), 3.58 (m, 12 H, $SCH_2CH_2N^+$), 3.82-3.87 (m, 18 H, OCH_2 and -$NMe_2CH_2CH_2OHI$), 5.31 (s, 6 H, O*H*), 6,03 (s, 3 H, $C_6H_3O_3$). ^{13}C-NMR: δ 6.8 (Si*Me*), 12.3 ($OCH_2CH_2CH_2CH_2Si$); 13.6 ($SiCH_2CH_2S$), 19.3 ($OCH_2CH_2CH_2CH_2Si$), 22.9 ($SCH_2CH_2N^+$), 26.3 ($SiCH_2CH_2S$), 32.1 ($OCH_2CH_2CH_2CH_2Si$), 50.3 (-$NMe_2CH_2CH_2OHI$), 54.5 (-$NMe_2CH_2CH_2OHI$), 63.1 ($SCH_2CH_2N^+$), 64.0 (-$NMe_2CH_2CH_2OHI$), 66.7 (OCH_2), 93.0 ($C_6H_3O_3$; *C*-H), 160.0 ($C_6H_3O_3$; *C*-O). ^{15}N-NMR: δ -324.3 (-*N*$Me_2CH_2CH_2OH$) ^{29}Si-NMR: δ 3.2 (G_1–*Si*Me). ESI: (2244.34 g/mol) q=2 (995.26 $[M\text{-}2I^-]^{2+}$), q=3 (621.55 $[M\text{-}3I^-]^{3+}$), q=4 (434.44 $[M\text{-}4I^-]^{4+}$), q=5 (321,97 $[M\text{-}5I^-]^{5+}$), q=6 (247.16 $[M\text{-}6I^-]^{6+}$). Anal. Calcd. $C_{69}H_{150}I_6N_6O_9S_6Si_3$ (2246.04 g/mol): C, 36.90; H, 6.73; N, 3.74; S, 8.57; Found: C, 36.51; H, 6.47; N, 3.66; S, 8.46.

4.3. Computational methods.

Computer atomistic models of dendrimers **14** and **17** were created (using Materials Studio software package from Accelrys Inc.) and parametrized. All dendrimers were consequently simulated in salt explicit water (TIP3P water model, 0.15 M of NaCl) for 65 ns under conditions T = 310 K and P = 0.1 MPa using Molecular Dynamics. All the equilibrated dendrimer structures from the last 30 ns of simulations were consequently analysed in terms of their size and density distribution of selected molecular components (radial distribution function). Electrostatic potential on molecular surface of the most representative dendrimer conformations was calculated/visualized (Adaptive Poisson-Boltzmann Solver, VMD). Please see the Supporting Information for more details.

4.4. pH titration.

A solution of NaOH (1.8 μM) was carefully added to a solution of **4** (38.5 mg) in water. The pH was measured using a pH-Meter Basic 20+ of Crison.

4.5. Antibacterial methodology.

The minimal inhibitory concentration (MIC) of the products was measured in 96-well tray microplates using the international standard methods ISO 20776-1 by microdilution tray preparations.[45] The assays were done in duplicate microplates with three different wells for each concentration analyzed in the microplate. The bacteria used in the analysis were *Escherichia coli* (CECT 515) (Gram-negative) and *Staphylococcus aureus* (CECT 240) (Gram-positive). Both strains were obtained from the "Colección Española de cultivos tipo" (CECT). A stock solution of the products was obtained by dissolving 0.01024 g of the compound with 10 ml of distilled water. After that, distilled water was added to obtain the desired concentration. The microplates were incubated at 37 ºC using an ultra microplate reader ELX808iu (Bio-Tek Instruments). The minimal bactericidal concentration (MBC) was calculated by inoculating 3 μl of the samples used to calculate the MIC in Petri dish with Mueller-Hinton agar. The samples were put on a drop in the plates. After 48 h of incubation at 37 ºC the presence of colonies was tested. The MBC was the minimal concentration in which not growth was detected.

For the stability experiments, the growth inhibition of the microorganisms was measured after the dendrimer was incubated in the different conditions. The software Statgraphics Centurion XV was used to make the Box-Behnken design.

5. Supporting Information

pH titration experiment of dendrimer **4** and theoretical calculation, description of synthesis of second and third generation dendrimers, selected NMR spectra.

6. Acknowledgments

This work has been supported by grants from CTQ2011-23245 (MINECO), and Consortium NANODENDMED ref S2011/BMD-2351 (CM). to University of Alcalá. This work was also supported by grants from the Ministerio de Educación for E.F.P. CIBER-BBN is an initiative funded by the VI National R&D&i Plan *2008-2011, Iniciativa Ingenio 2010, Consolider Program, CIBER Actions* and financed by the Instituto de Salud Carlos III with assistance from the *European Regional Development Fund*.

7. References

1. A. Coates, Y. M. Hu, R. Bax and C. Page, 2002, **1**, 895-910.
2. M. Tischer, G. Pradel, K. Ohlsen and U. Holzgrabe, *Chem. Med. Chem.*, 2012, **7**, 22-31.
3. E. R. Kenawy, F. I. Abdel-Hay, A. E. R. R. El-Shanshoury and M. H. El-Newehy, *J. Polym. Sci. Part A: Polym. Chem.*, 2002, **40**, 2384–2393.
4. R. B. Tompkin, *Food Technol.*, 1984, **38**, 226-226.
5. A. Muñoz-Bonilla and M. Fernández-García, *Prog. Polym. Sci.*, 2012, **37**, 281-339.
6. X. Liu, P. Rocchi and L. Peng, *New J. Chem.*, 2012, **9**, 256-263.
7. J. L. Jiménez, M. Pion, F. J. de la Mata, R. Gómez, E. Muñoz, M. Leal and M. A. Muñoz-Fernández, *New J. Chem.*, 2012, **36**, 299-309.
8. A. J. L. Villaraza, A. Bumb and M. W. Brechbiel, *Chem. Rev.*, 2010, **110**, 2921–2959.
9. P. M. H. Heegaard, U. Boas and N. S. Sorensen, *Bioconjugate Chem.*, 2010, **21**, 405-418.
10. S. Svenson, *Eur. J. Pharm. Biopharm.*, 2009, **71**, 445-462.
11. D. G. Shcharbin, B. Klajnert and M. Bryszewska, *Biochemistry*, 2009, **74**, 1070-1079.
12. O. Rolland, C. O. Turrin, A. M. Caminade and J. P. Majoral, *New J. Chem.*, 2009, **33**, 1809-1824.
13. N. Joshi and M. Grinstaff, *Curr. Top. Med. Chem.*, 2008, **8**, 1225-1236.
14. B. Dizman, M. O. Elasri and L. J. Mathias, *J. Appl. Polym. Sci.*, 2004, **94**, 635-642.
15. S. Hou, C. Zhou, Z. Liu, A. W. Young, Z. Shi, D. Ren and N. R. Kallenbach, *Bioorg. Med. Chem. Lett.*, 2009, **19**, 5478-5481.
16. T. Osamura, M. Ozawa and T. Iwama, *Patent JP2011037716A*, 2011.
17. T. Ikeda, H. Hirayama, H. Yamaguchi, S. Tazuke and M. Watanabe, *Antimicrob. Agents Chem.* , 1986, **30**, 132-136.
18. J. L. Jimenez, M. I. Clemente, N. D. Weber, J. Sanchez, P. Ortega, l. M. F. J. de, R. Gomez, D. Garcia, L. A. Lopez-Fernandez and M. A. Munoz-Fernandez, 2010, **24**, 331-343.
19. I. Posadas, B. Lopez-Hernandez, M. I. Clemente, J. L. Jimenez, P. Ortega, l. M. J. de, R. Gomez, M. A. Munoz-Fernandez and V. Cena, 2009, **26**, 1181-1191.
20. J. F. Bermejo, P. Ortega, L. Chonco, R. Eritja, R. Samaniego, M. Muellner, J. E. de, d. l. M. F. Javier, J. C. Flores, R. Gomez and A. Munoz-Fernandez, 2007, **13**, 483-495.
21. P. Ortega, M. Cobaleda, J. M. Hernández-Ros, E. Fuentes-Paniagua, J. Sánchez-Nieves, M. P. Tarazona, J. L. Copa-Patiño, J. Soliveri, F. J. de la Mata and R. Gómez, *Org. Biomol. Chem.*, 2011, **9**, 5238-5248.
22. B. Rasines, J. M. Hernandez-Ros, l. C. N. de, J. L. Copa-Patino, J. Soliveri, M. A. Munoz-Fernandez, R. Gomez and l. M. F. J. de, 2009, 8704-8713.
23. M. J. Kade, D. J. Burke and C. J. Hawker, *J. Polym. Sci., Part A: Polym. Chem.*, 2010, **48**, 743-750.
24. B. H. Northrop and R. N. Coffey, *J. Am. Chem. Soc.*, 2012, **134**, 13804–13817.
25. C. E. Hoyle and C. N. Bowman, *Angew. Chem. Int. Ed.*, 2010, **49**, 1540-1573.
26. A. B. Love, *Polym. Chem.*, 2010, **1**, 17–36.

27. J. Mergy, A. Fournier, E. Hachet and R. Auzely-Velty, 2012, **50**, 4019-4028.
28. V. Darcos, S. Antoniacomi, C. Paniagua and J. Coudane, 2012, **3**, 362-368.
29. C. Rissing and D. Y. Son, *Main Group Chem.*, 2009, **8**, 251-262.
30. K. L. Killops, L. M. Campos and C. J. Hawker, *J. Am. Chem. Soc.*, 2008, **130**, 5062–5064.
31. T. Kang, R. J. Amir, A. Khan, K. Ohshimizu, J. N. Hunt, K. Sivanandan, M. I. Montáñez, M. Malkoch, M. Ueda and C. J. Hawker, *Chem. Commun.*, 2010, **46**, 1556-1558.
32. M. I. Montañez, L. M. Campos, P. Antoni, Y. Hed, M. V. Walter, B. T. Krull, A. Khan, A. Hult, C. J. Hawker and M. Malkoch, *Macromolecules*, 2010, **43**, 6004–6013.
33. C. Nilsson, E. Malmström, M. Johansson and S. M. Trey, *J. Polym. Sci., Part A: Polym. Chem.*, 2009, **47**, 589–601.
34. C. Rissing and D. Y. Son, *Organometallics*, 2009, **28**, 3167-3172.
35. L. Chen, T. E. Andersson, C. Rissing, S. Yang, S. Chen and D. Y. Son, *J. Mat. Chem. B*, 2013, **1**, 116-122. .
36. C. Rissing and D. Y. Son, *Organometallics*, 2008, **27**, 5394-5397.
37. S. W. Krska and D. Seyferth, 1998, **120**, 3604-3612.
38. E. Pedziwiatr-Werbicka, E. Fuentes-Paniagua, V. Dzmitruk, J. Sánchez-Nieves, M. Sudas, E. Drozd, A. Shakhbazau, D. Shcharbin, F. J. d. l. Mata, R. Gómez-Ramírez, M. Á. Muñoz-Fernández and M. Bryszewska, *Colloids Surf. B: Biointerfaces*, 2013, **109**, 183– 189.
39. B. Heldreth and E. Turos, *Curr. Med. Chem.*, 2005, **4**, 295-315.
40. S. Kim, R. Kubec and R. A. Musah, *J. Ethnopharm.*, 2006, **104**, 188-192.
41. H. Tapiero, D. M. Townsend and K. D. Tew, *Biomed. Pharmacother.*, 2004, **58**, 183-193.
42. J. Sánchez-Nieves, P. Ortega, M. Á. Muñoz-Fernández, R. Gómez and F. J. de la Mata, *Tetrahedron*, 2010, **66**, 9203-9213.
43. E. Fuentes-Paniagua, C. E. Peña-González, Marta Galán, R. Gómez, F. J. d. l. Mata and J. Sánchez-Nieves, *Organometallics*, 2013, **32**, 1789−1796.
44. C. Z. Chen, N. C. Beck-Tan, P. Dhurjati, T. K. van Dyk, R. A. LaRossa and S. L. Cooper, *Biomacromolecules*, 2000, **1**, 473−480.
45. *Reference Methods for the testing the "in vitro" activity of antimicrobial agents against bacteria involved in infectious diseases (ISO 20776-1)*, 2006.